

On the generation and propagation of Makran swells in the Arabian Sea

T.R. Anoop^{1,2,3}, P.R. Shanas⁴, V.M. Aboobacker^{4*}, V. Sanil Kumar², L. Sheela Nair¹, R. Prasad¹, S. Reji¹

¹ESSO-National Centre for Earth Science Studies, Ministry of Earth Science,
Trivandrum, Kerala-695011, India

²Ocean Engineering Division, CSIR-National Institute of Oceanography
(Council of Scientific & Industrial Research), Dona Paula, Goa 403 004, India

³Bharathidasan University, Tiruchirappalli 620023 Tamil Nadu, India

⁴Faculty of Marine Sciences, Department of Marine Physics,
King Abdulaziz University, Jeddah, Saudi Arabia

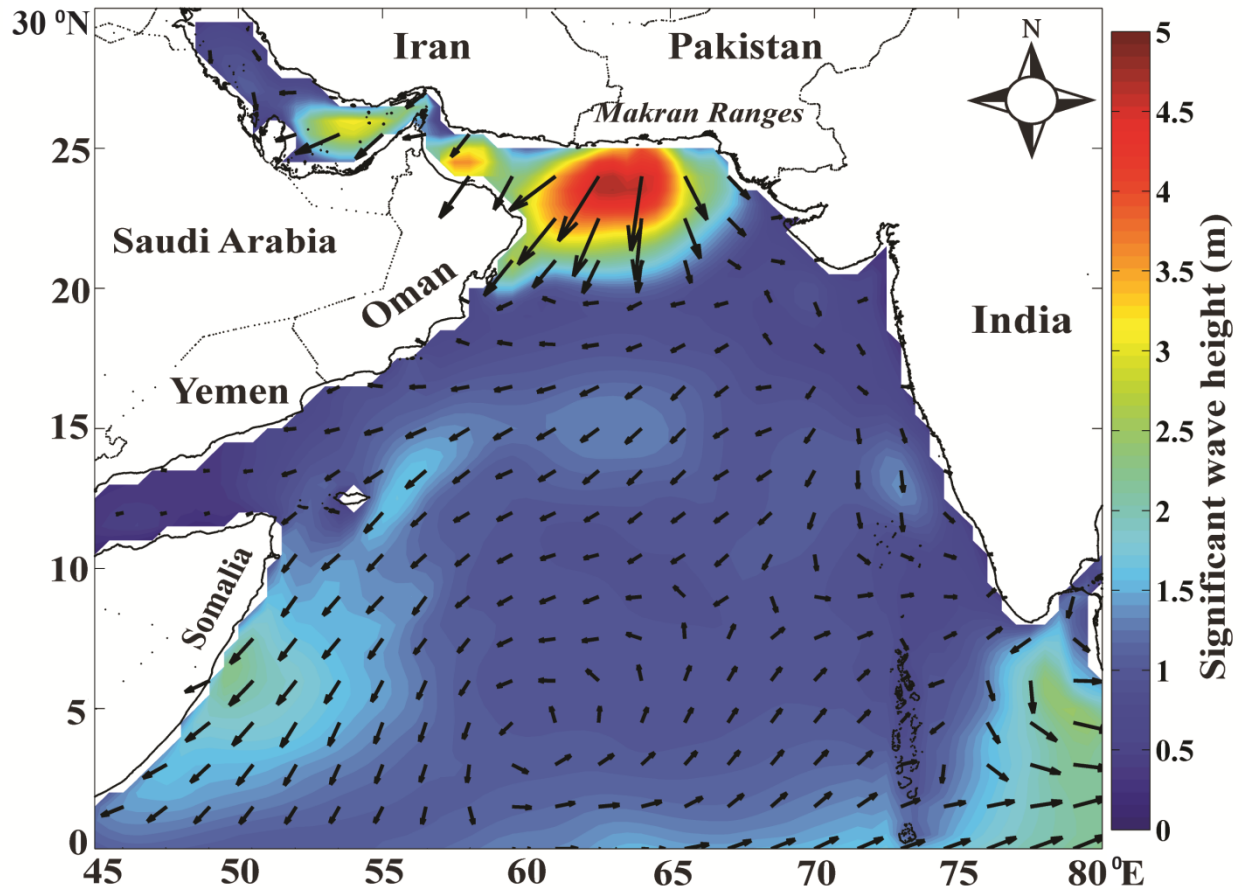
*email: vmabacker@gmail.com

Abstract

Persistent and periodic northerly low-level jets have been identified in the South Asian mid-latitudes and sub-tropics, which are modified by the presence of Makran mountain ranges adjacent to the central south coast of Pakistan, where they blow predominantly in the west-northwest to northeast directions. These winds lead to the generation of a new wave system and propagate through the Arabian Sea as “makran swells”. They are prevalent during October to May. The measurements along the west coast of India reveal systematic variations in the wave spectra relating the makran events. This has been further verified through the WaveWatch III simulations forced by the CFSR winds. The significant wave heights up to 4.5 m were hindcasted in the northern Arabian Sea during these events. Once generated, the makran swells propagate to the eastern Arabian Sea and western Arabian Sea with directional sectors of 300° - 360° and 0° - 60°, respectively. The characteristic features and the spatial extension of the makran swells are particularly analysed.

Key words: Low level jet; Makran swells; Arabian Sea; Shamal swells; Significant wave height; Monsoon

Graphical Abstract



The dynamics leading to the generation of makran swells in the Arabian Sea have been discussed. Evidences of makran swells were identified in the measurements along the west coast of India. Wave hindcasting have been carried out to describe the propagation patterns of makran swells in the Arabian Sea.

1. Introduction

The wind systems in the Arabian Sea are controlled by various factors that include the dynamics involved and the region of formation and propagation. The low level jets (LLJ) are the most influencing wind systems that affect the ocean surface. The Findlater jet is the basis for southwest (SW) monsoon winds (Findlater, 1969). It is the prime wind system in the North Indian Ocean during the boreal summer, which blows predominantly in southwest direction. The northeast (NE) monsoon winds – the second major wind system in the Arabian Sea are associated with the southward movement of the Continental Tropical Convergence Zone (CTCZ) during the withdrawal phase of summer monsoon (Rajeevan et al., 2012). The northerly LLJ originated from the Middle East, known as shamal winds, has significant influence in the Arabian/Persian Gulf during summer and winter (Perrone, 1979; Yu et al., 2016). They are evolved by the dynamic interaction of upper air jet streams and distribution of lower tropospheric pressure zones. It often extends to the Arabian Sea, especially during pre- and post-monsoon seasons and weak SW monsoon periods, and has a liable impact on the surface wave characteristics (Aboobacker et al., 2011a; Vinodkumar et al., 2014; Aboobacker et al., 2018a, 2018b). The summer shamal winds are prominently restricted to the Gulf of Oman region because of strong SW monsoon winds in the Arabian Sea. In addition to the above wind systems, the sea and land breeze systems along the coastal regions of west India are most effective during pre-monsoon periods (Aparna et al., 2005).

A recent study identifies the existence of a South Asian northerly low-level jet (LLJ) at regular intervals throughout the year (Aboobacker and Shanas, 2018a; Anoop et al., 2019). It is caused by the synoptic high in the mid-latitudes and the synoptic low in the subtropics. A schematic representation on the formation of this LLJ is illustrated in Figure 1a. The core is situated at 850 hPa in western Afghanistan and its propagation is predominantly towards the south over the subtropical terrains (27° - 35° N, 62° - 66° E). This wind system is further modified and redistributed by the presence of the Makran mountain ranges in southern Pakistan (Figure 1b). During SW monsoon (Jun – Sep), its propagation in the Arabian Sea is restricted by the stronger SW monsoon LLJ, while it is prevalent during October to May. The surface wind system thus evolved in the southern coast of Pakistan and in the Arabian Sea is named as makran winds (Aboobacker and Shanas, 2018a). Off the central south coast of Pakistan, the makran wind

speed ranges up to 20 m/s in the north direction. As propagates through the Arabian Sea, it diverges to two predominant directional sectors – 300° to 360° (WNW – N) and 0° to 60° (N-ENE). It has sensible impacts in the eastern Arabian Sea and western Arabian Sea, where the magnitudes are generally between 6 m/s and 14 m/s. These winds can influence the surface currents and the general circulations in the Arabian Sea, as identified by Samiksha et al. (2014) when the shamal winds are prevailing.

The sea state characteristics and the controlling factors in the Arabian Sea were investigated comprehensively (e.g., Anoop et al., 2016; Samiksha et al., 2012; Aboobacker et al., 2011 a, b). The SW and NE monsoon winds are the major forcings in the Arabian Sea; thereby generates large/moderate waves depending on the intensity of the wind systems. During SW monsoon, the average significant wave height in the Arabian Sea lies in the range 3.0 – 3.5 m, while it is less than 2.0 m during the other seasons (Anoop et al., 2015). The swells that propagated from the Southern Ocean and South Indian Ocean frequently interact with the wind seas/young swells in the Arabian Sea, which lead to significant modifications in the total wave conditions (Kumar et al., 2012; Vethamony et al., 2011). Such interactions are prevalent during non-SW monsoon seasons (Kumar et al. 2012; Glejin et al., 2013b; Vethamony et al., 2011). Samiksha et al. (2012) verified the propagation of Atlantic Ocean swells in the north Indian Ocean by analyzing a cyclone event occurred in the southern tip of South Africa, which forms the waves up to 15.0 m heights in the generation area. The phenomenon of Kallakkadal – a long period swell observed along the southwest coast of India was traced back to its generation area in the south Indian Ocean (Remya et al., 2016). The shamal swells, generated in the Arabian Sea due to the effect of shamal winds, have a prominent role on the wave characteristics in the Arabian Sea during pre- and post-monsoon seasons and weak SW monsoon periods (Aboobacker et al., 2011a; Glejin et al, 2013a). They generate large waves up to 4.0 m in the northern Arabian Sea and propagate to the west coast of India as shamal swells. The sea breeze during pre-monsoon season modifies the wave conditions along the west coast of India (Glejin et al., 2013b; Aboobacker et al., 2014). Despite the vast investigations on the wave characteristics in this region, the role of makran swells in the Arabian Sea is yet to be explored. In this study, we aim to investigate the generation and propagation of makran swells, their interaction with the southerly swells and their spatial extension in the Arabian Sea.

2. Area of study

The Arabian Sea is a semi-enclosed basin situated in the western North Indian Ocean, bounded by the Indian subcontinent in the east, Pakistan and Iran in the north, and Oman, UAE, Yemen and Somalia in the west (Figure 1a). The Gulf of Oman and the Gulf of Aden are the two major Gulfs in the Arabian Sea; the former connects to the Arabian/Persian Gulf through the Hormuz Strait, while the latter connects to the Red Sea through the Bab-el-Mandeb Strait. The maximum depth of the Arabian Sea is around 4600 m. The continental shelf in the eastern Arabian Sea is relatively wide and shallow, while that in the western Arabian Sea is narrow and deeper. The seasons are particularly classified in to three: pre-monsoon (Feb-May), SW monsoon (Jun-Sep) and NE monsoon (Oct-Jan) (Aboobacker et al., 2011a). The SW monsoon winds have high impact in the Arabian Sea than those winds during the other seasons. We refer the pre-monsoon and NE monsoon seasons in this study as non-SW monsoon seasons. The shamal and makran winds can be considered as extreme wind conditions in the northern Arabian Sea during non-SW monsoon months (Aboobacker & Shanas, 2018a). These winds have a certain impact on the wave characteristics in the Arabian Sea.

3. Data and methodology

The wave data has been collected at five nearshore locations along the west coast of India using directional wave rider buoys (locations are shown in Figure 1a). The measurement locations are Ratnagiri (13m depth), Karwar (15m depth), Honnavar (9m depth), Calicut (22m depth) and Quilon (22m depth), which extend ~1000 km coastal belt. The data were collected for every 30 minutes during February 2014 - January 2015 at Calicut and Quilon, and January 2012 - December 2014 at Honnavar, Karwar and Ratnagiri, and derived the spectral and integral wave parameters using the method described by Tucker (1989).

The wave simulations have been carried out for a period of 7.5 years (2011-2018) using WaveWatch III (hereafter, WW3), a third generation spectral wave model (Tolman, 2014). The description on WW3 is amply described in the literature. The ST4 physics scheme (Ardhuin et al., 2010), which is found suitable in swell dominant wave conditions (e.g., Bi et al., 2015), has been applied here. The model domain covers the entire Indian Ocean (30° – 110° E; 60° S– 35° N) considering a spatial resolution of $0.5^{\circ} \times 0.5^{\circ}$. A one-way nesting is applied for the north Indian Ocean (30° – 110° E; 0 - 35° N) with a spatial resolution of $0.1^{\circ} \times 0.1^{\circ}$. The bathymetry is

derived using the 30- arc second GEBCO datasets. The wave frequencies have been discretized logarithmically from 0.04 to 0.86 Hz that accounts 36 bins. The wave directions have been discretized into 36 bins with an interval of 10° . The wave model has been forced with the surface wind velocities from the Climate Forecast System Reanalysis (CFSR), which are available for every 1 hour with a spatial resolution of $0.312^\circ \times 0.312^\circ$ (1979-2010) and $0.205^\circ \times \sim 0.204^\circ$ (2011 onwards) (Saha et al., 2014). The CFSR winds have been used worldwide in wave hindcasting studies (e.g., Chawla et al., 2013; Bao & Zhang, 2013; Sharp et al., 2015). We obtained a reasonable statistic for the CFSR wind speeds when compared with the GlobWave data using Altwave toolbox (Appendini et al., 2014) in the Arabian Sea: correlation coefficient = 0.92, bias = 0.32, r.m.s. error = 1.43 and scatter index = 0.20. The wave parameters - significant wave height (H_s), mean wave period (T_{m02}), peak wave period (T_p) and mean wave direction (θ) were derived for every 3 hours from the modelled wave spectra. The model validation and the important results are discussed in the following sections.

4. Model validation

The model results have been validated with the buoy measurement at Ratnagiri for 1-year period from January to December 2012. We obtained significant correlation (0.97) for H_s with measurement and reasonable other statistics. For wave period, the correlation coefficient obtained is 0.80 with SI of 0.15. The r.m.s error for H_s and T_m is 0.19 m and 0.74 s respectively. Considering the wide ranges of wave heights and periods obtained in the Arabian Sea, these r.m.s. errors are well within the reasonable limits.

5. Results and discussion

The model hindcast clearly reproduces the makran swells in the Arabian Sea. A total of 53 events were identified during the study period based on the following criterion: (i) The dominant wave directions are from WNW to NE, which is aligned with the makran wind events and by allowing temporal lags required for wave generation and propagation and (ii) a persistent duration of atleast 12 hours in each event for the waves with above specifications. Since the primary aim of the study is to characterize the makran swells in the Arabian Sea, we picked only a few major events to distinguish and discuss the features.

The shamal wind system is originating from the Arabian Peninsula (Perrone, 1979), while the makran wind system originates in the western Afghanistan (Figure 1b), although both are considered as northerly LLJs. Their existences in the Arabian Sea are in the same seasons, but differ in their period of prevalence. They may occur independently or concurrently. The independent events are generally stronger than the concurrent events. The shamal wind/wave weakens the northeasterly component of makran wind/wave, while the northwest component merge with shamal wind/wave as it blows towards the northwest coast of India, when they occur concurrently. The potential generation areas of shamal swells are the Gulf of Oman and the east coast of Oman (Aboobacker et al., 2011a), while those of makran swells are in the northern Arabian Sea off the south coast of Pakistan. The makran swells observed along the west coast of India have a resemblance with the shamal swells in terms of the magnitude and frequency, however, the shamal swells are predominantly from WNW/NW (a shift of 15° - 25° with the dominant makran swells), which is due to the differences in the wind distribution and wave generation areas.

5.1. Generation and propagation of makran swells

The measured wave spectra at select locations along the west coast of India during a non-monsoon period (Feb 2014) reveal the presence of two distinct swell systems – (i) long-period swells (< 0.12 Hz) propagated from the South Indian Ocean in S-SW direction and (ii) moderate swells ($0.12 - 0.25$ Hz) propagated from the northern Arabian Sea in NNW direction (Figure 2a-c). The southerly/southwesterly swells are common along the west coast of India, which are persistent throughout the year (Aboobacker et al., 2011b; Vethamony et al., 2011; Glejin et al, 2013b). The NNW swells are associated with the makran winds (hereby named as makran swells). During the makran events, the pre-existing southwesterly swell in the northern Arabian Sea has been weakened and a strong northerly wave system has been developed. Its growth and propagation is controlled by the intensity and duration of makran winds. It is propagating in two dominant directional sectors – (i) WNW to NNW and (ii) N to NE. Typically, the makran events have durations between 1 to 6 days. The makran swell spectral densities are higher in Ratnagiri and lower in Quilon with the peak energy frequencies of 0.22 Hz and 0.18 Hz, respectively (Figure 2c). This indicates that the intensity and duration of the makran swells decreases from north to south along the west coast of India. The maximum H_s at Ratnagiri, Karwar, Honnavar, Calicut and Quilon associated with makran swells are 1.47 m, 1.55 m, 1.26 m, 0.90 m and 0.86

m, respectively. The corresponding T_{m02} are 6.0 s, 6.5 s, 6.9 s, 7.0, 7.1 s, respectively, which are consistent with shamal swell periods (Aboobacker et al., 2011a). Although these periods are relatively low, they follow the definition of swells as these waves are propagated out of the generation area to a large distance in absence of the corresponding winds. Similar low period swells were identified along the west coast of India during SW monsoon when the potential swell generation area is in the southwestern Arabian Sea (Aboobacker et al., 2011b). The maximum H_s is in the central west coast (Karwar), although the percentage of occurrence is relatively high at Ratnagiri. This discrepancy is attributed to the bathymetry of the region, i.e., the continental shelf of Ratnagiri is wider than that of Karwar, hence, relatively large dissipation is expected along the coast of Ratnagiri. The southwesterly swells are very low or almost negligible during the active makran events. Due to the shallow water effects, the makran swells along these coasts have a shore normal propagation, which leads to a shift of $30^\circ - 45^\circ$ from the dominant makran direction (transformation from NNW to NW/WNW). Considering the generation area of the central south coast of Pakistan and the mean period of propagation as 6.0 s, these swells will reach the Ratnagiri coast in ~ 37 hours and the Quilon coast in ~ 63 hours. Hence, there is a time lag of ~ 26 hours between these two stations having a distance of ~ 1000 km. Although relatively low, the spectral densities of the wind seas generated by the sea breeze - land breeze system are also apparent in all the coastal stations, which maintain the diurnal variability (Aboobacker et al., 2014).

The analysis has been extended further using the wave model results. Figure 3 shows the snapshots of the makran swells generated and propagated in the Arabian Sea during 07 - 08 Feb 2014. This is a moderate makran event. Here the makran swells generated in the northern Arabian Sea has H_s up to 1.8 m with two distinct directional sectors of propagation as discussed above. The NW/NNW makran swells reach the entire the west coast of India with a decreasing order of H_s from north to south. In the central west coast of India, the makran swells have H_s up to 1.3 m, which is $\sim 28\%$ reduction with that in the northern Arabian Sea. In the southwest coast of India (the Kerala coast), the reduction in H_s is around $50\% - 55\%$. The NE/NNE makran swells experiences all along the Oman coast, with relatively high intensity in the eastern coasts. They occasionally reach the coast of Somalia. Similar to the central west coast of India, the makran swells have a reduction of around $25\% - 30\%$ in H_s in the east coast of Oman. The N makran swells propagate to the central Arabian Sea until it weakens or merges with the southerly

swells. A noticeable feature during the evolution of the makran swells is that the southerly swells weaken as the makran swells dominate.

In combination with the shamal swells and southerly swells, there are typically five scenarios in the Arabian Sea: (i) independent shamal swells, (ii) independent makran swells, (iii) dominance of makran swells over shamal swells or vice versa, (iv) co-existence of both shamal and makran swells and (v) interaction of makran swells with the southerly swells. We refer Aboobacker et al (2011a) for a detailed description on the first scenario; however, we used them for inter-comparisons in this discussion. The remaining scenarios have been addressed in the following sub-sections. These cases are chosen from the simulation period according to the prevalence of makran/shamal winds and the corresponding waves in the Arabian Sea.

5.2. Case 1: Independent makran swells

The results show that there are stronger makran swells in the Arabian Sea; most of them are associated with independent makran events, as they control the wind system in the northern Arabian Sea when such swells are observed. In this case, the region of prevalence of makran winds are relatively wider, often extends up to the Gulf of Oman and part of the Arabian/Persian Gulf. Figure 4a shows the evolution of the independent makran swells in the Arabian Sea with maximum intensity during the study period. Prior to the makran event (say, on 27 Dec 2012), the waves in the Arabian Sea are weaker with the H_s of the order of 0.5 - 1.5 m. In the next 24 hours, the makran swells evolved with H_s up to 4.5 m, 3.5 m, 3.0 m in the northern Arabian Sea, the Gulf of Oman and the Arabian Gulf respectively. The wave direction is typically off the makran winds. Although the makran swells in the Gulfs weaken within a day, those in the Arabian Sea continue for 3 – 4 days. The propagation and gradual decrease (spatially and temporally) of makran swell energies are clearly evident. The NNE/NE component of the makran swells continues up to the western equatorial Indian Ocean.

5.3. Case 2: Dominance of makran swells over shamal swells

We analysed the wave patterns when both makran events and shamal event occur concurrently. In such cases, the swells generated by these systems have different features; either one of them dominates or both are in similar magnitudes. The dominance of makran swells over shamal swells or vice versa differs according to their intensities and region of prevalence. In some cases, the shamal events occur prior to or along with the makran events. However, when the makran

winds are stronger than the shamal winds, the pre-/co-existing shamal swells in the Arabian Sea weakens, and yields to a clear dominance of makran swells. Figure 4b illustrates such an event in the Arabian Sea with maximum intensity during the study period, in which the shamal swells are present in the Gulf of Oman upon the generation of the makran swells, which has been weakened within the next 24 hours. Here, the shamal H_s were of the order of 1.5 – 2.0 m, while the makran H_s are up to 4.0 m. The propagation and spatial extension patterns of the Case 2 makran swells are similar to the Case 1 makran swells.

Dominance of shamal swells over the makran swells also occurs during the strongest shamal events in the Arabian Sea. Aboobacker et al (2011a) identified one of the strongest shamal swells in the Arabian Sea during 02-04 Feb 2008. Although it was not known, a close analysis of Figure 4a in the above paper indicates that there exist makran swells off the central south coast of Pakistan with relatively lower wave heights. Due to the dominance of shamal swells, major part of the makran swells were converged to the shamal swells and propagated to the west coast of India in WNW-NNW directions. We find similar features in a few other occasions.

5.4. Case 3: Co-existence of makran and shamal swells

At particular cases, the shamal and makran swells co-exist in the Arabian Sea in equal magnitudes, contributed by the corresponding wind systems. We picked one of such event with maximum intensity during the study period. In such cases, the swells in the northern Arabian Sea is relatively weaker compared to Case 1 and Case 2. There is a component of shamal swells in the southeast coast of Oman – around 17° N (Aboobacker et al., 2011a), which gets modified by the NNE/NE makran swells that leads to a higher wave heights in the southwestern Arabian Sea (Figure 4c). In this case, the H_s is larger in the coast of Somalia. The propagation and spatial extension patterns of the Case 3 makran swells are slightly different from the Case 1 and Case 2 makran swells. The NW/NNW component of the makran swells propagate only up to the central west coast of India with relatively low H_s , while the NNE/NE component along with the shamal swells and part of the NE monsoon waves reaches the Somalia coast with relatively higher H_s (up to 3.5 m) than the Case 1 and Case 2 makran swells in this region.

5.5. Interaction with southerly swells

The long-period swells propagating from the south Indian Ocean or the Southern Ocean are present in the north Indian Ocean throughout the year, although their intensity varies according

to the storm events in their generation area (Anoop et al., 2015; Samiksha et al., 2012; Aboobacker et al., 2011b). They are approaching in the central and western Arabian Sea in a dominant southerly direction. Along the west coast of India, they tend to move in a south-southwesterly direction. They prevail in the Arabian Sea when the regional wind systems are weak, especially during non-SW monsoon months. However, along the coastal regions they interact with local wind seas generated by sea breeze and land breeze (Vethamony et al., 2011).

The makran swells and the southerly swells are merely in opposite directions. They interact with each other and result in distinct characteristics (see Figure 3 and Figure 4). The most featured interaction is between the high energy northerly components of makran swells meet the low energy southerly swells in the central Arabian Sea. As a result, the southerly swell weakens and the resultant wave shifts to approx. 45° and propagates towards the southwestern Arabian Sea as northeasterly waves (Figure 3). Spatially and temporally, it is a gradual weakening of southerly swells when the makran event prevails in the Arabian Sea. For instance, the signatures of pre-existing southerly swells are clearly visible at 18:00 hours on 07 Feb 2014 in the central western Arabian Sea and in the Gulf of Oman, which are gradually diminished within the next few hours. Along the west coast of India, the northwest component of makran swells meets the south-southeasterly swells and the resultant wave continues in a northwest/north-northwest direction, with a slight deviation (Figure 4b). In particular cases, stronger southerly swells generated due to storms in the western tropical south Indian Ocean interact with the makran swells, as also evident in Figure 3 and Figure 4c. The resultant waves thus formed converge to a common easterly direction and propagates towards the coast with a relative increase in wave heights, as seen in the southwestern Arabian Sea (around 8° N). These types of interactions may have large oceanographic implications such as in air sea interaction, ocean mixing etc.

6. Conclusions

The makran winds generate the makran swells in the northern Arabian Sea and propagate in the Arabian Sea in varying directions. They are prevalent during the non-monsoon seasons. The measurements along the west coast of India indicate that the makran swell energy densities are in the frequency interval between 0.12 and 0.25 Hz. The intensity and duration of makran swells decreases from north to south along the west coast of India. The wave hindcast shows that the makran swells propagate to the western Arabian Sea and the eastern Arabian Sea in NNE-ENE

and WNW-NNW directions, respectively, where they dissipate along the bounded coastal regions. The N component of the makran swells propagates to the central Arabian Sea until it converges to the southerly swells. Three typical cases of makran events were identified according to the intensity of the makran swells. The independent makran swells results with higher wave heights than the other two cases – the dominance of makran swells over shamal swells and their co-existence. The makran swell H_s reaches up to 4.5 m in the northern Arabian Sea, while gradually decreases when it propagates southwards in the Arabian Sea. The makran events can be considered as one among the extreme events in the northern Arabian Sea during non-monsoon months. However, a climatological investigation is required to substantiate this, which is under consideration.

Acknowledgements

The authors acknowledge the directors of ESSO-NCESS, Kerala, CSIR-NIO, Goa of Government of India and Deanship of Scientific Research, King Abdulaziz University, Jeddah, Saudi Arabia for providing encouragement to carry out the study. CSIR, New Delhi for funding the wave measurement at Honnavar and ESSO-INCOIS, Ministry of Earth Sciences, Government of India for funding the wave measurement at Ratnagiri, Karwar, Calicut and Quilon. T. M. Balakrishnan Nair, Arun N, Jayakumar, S, J. Singh, E.K. Sarath Raj, Syam Shankar, Vishnu S, Muhammed Asif, provided support during data collection. This work forms part of the Ph.D. thesis of the first author registered at Bharathidasan University, Tiruchirappalli.

References

- Aboobacker, V. M., Vethamony, P., & Rashmi, R. (2011a). “Shamal” swells in the Arabian Sea and their influence along the west coast of India. *Geophysical Research Letters*, 38(3). <https://doi.org/10.1029/2010GL045736>
- Aboobacker, V. M., Rashmi, R., Vethamony, P., & Menon, H. B. (2011b). On the dominance of pre-existing swells over wind seas along the west coast of India. *Continental Shelf Research*, 31(16), 1701-1712. <https://doi.org/10.1016/j.csr.2011.07.010>
- Aboobacker, V. M., Seemanth, M., Samiksha, S. V., Sudheesh, K., Kerkar, J., & Vethamony, P. (2014). Sea breeze-induced wind sea growth in the central west coast of India. *Ocean Engineering*, 84, 20-28. <https://doi.org/10.1016/j.oceaneng.2014.03.030>

- Aboobacker, V. M., & Shanas, P. R. (2018a). The climatology of shamals in the Arabian Sea—Part 1: Surface winds. *International Journal of Climatology*, 38(12), 4405-4416. <https://doi.org/10.1002/joc.5711>
- Aboobacker, V. M., & Shanas, P. R. (2018b). The climatology of shamals in the Arabian Sea—Part 2: Surface waves. *International Journal of Climatology*, 38(12), 4417-4430. <https://doi.org/10.1002/joc.5677>
- Anoop, T. R., Unnikrishnan, C. K., Ashok, K., Ramachandran, K. K., & Prakash, T. N. (2019). Periodic low level jet in south west Asia: Influence on regional hydrology and aerosol optical depth. (Under Review, *Current Science*)
- Anoop, T. R., Kumar, V. S., Shanas, P. R., Johnson, G. (2015). Surface Wave Climatology and Its Variability in the North Indian Ocean Based on ERA-Interim Reanalysis. *Journal of Atmospheric and Oceanic Technology*, 32, 1372–1385. <https://doi.org/10.5194/os-12-369-2016>. doi/pdf/10.1175/JTECH-D-14-00212.1
- Anoop, T. R., Kumar, V. S., Shanas, P. R., Johnson, G., & Amrutha, M. M. (2016). Indian Ocean Dipole modulated wave climate of eastern Arabian Sea. *Ocean Science*, 12, 2473–2496. <https://doi.org/10.5194/os-12-369-2016>
- Aparna, M., Shetye, S.R., Shankar, D., Shenoi, S.S.C., Mehra, P., Desai, R.G.P. (2005). Estimating the seaward extent of sea breeze from QuikSCAT scatterometry. *Geophysical Research Letters*. 32(L13601). <https://doi.org/10.1029/2005GL023107>
- Appendini, C. M., Torres-Freyermuth, A., Salles, P., López-González, J., & Mendoza, E. T. (2014). Wave climate and trends for the Gulf of Mexico: A 30-yr wave hindcast. *Journal of Climate*, 27(4), 1619-1632. <https://doi.org/10.1175/JCLI-D-13-00206.1>
- Ardhuin, F., Rogers, E., Babanin, A. V., Filipot, J. F., Magne, R., Roland, A., ... & Collard, F. (2010). Semiempirical dissipation source functions for ocean waves. Part I: Definition, calibration, and validation. *Journal of Physical Oceanography*, 40(9), 1917-1941. <https://doi.org/10.1175/2010JPO4324.1>
- Bao, X., & Zhang, F. (2013). Evaluation of NCEP–CFSR, NCEP–NCAR, ERA-Interim, and ERA-40 reanalysis datasets against independent sounding observations over the Tibetan Plateau. *Journal of Climate*, 26(1), 206-214. <https://doi.org/10.1175/JCLI-D-12-00056.1>
- Bi, F., Song, J., Wu, K., & Xu, Y. (2015). Evaluation of the simulation capability of the Wavewatch III model for Pacific Ocean wave. *Acta Oceanologica Sinica*, 34(9), 43-57. <https://doi.org/10.1007/s13131-015-0737-1>
- Chawla, A., Spindler, D. M., & Tolman, H. L. (2013). Validation of a thirty year wave hindcast using the Climate Forecast System Reanalysis winds. *Ocean Modelling*, 70, 189-206. <https://doi.org/10.1016/j.ocemod.2012.07.005>

- Findlater, J. (1969). A major low-level air current near the Indian Ocean during the northern summer. *Quarterly Journal of the Royal Meteorological Society*, 95(404), 362-380. <https://doi.org/10.1002/qj.49709540409>
- Glejin, J., Kumar, V. S., Nair, T. B., Singh, J., & Mehra, P. (2013a). Observational evidence of summer Shamal swells along the west coast of India. *Journal of Atmospheric and Oceanic Technology*, 30(2), 379-388. <https://doi.org/10.1175/JTECH-D-12-00059.1>
- Glejin, J., Sanil Kumar, V., Nair, B., & Singh, J. (2013b). Influence of winds on temporally varying short and long period gravity waves in the near shore regions of the eastern Arabian Sea. *Ocean Science*, 9(2), 343-353. <https://doi.org/10.5194/os-9-343-2013>
- Kumar, V. S., Johnson, G., Dora, G. U., Chempalayil, S. P., Singh, J., & Pednekar, P. (2012). Variations in nearshore waves along Karnataka, west coast of India. *Journal of earth system science*, 121(2), 393-403. <https://doi.org/10.1007/s12040-012-0160-3>
- Perrone, I.J. (1979). Winter Shamal in the Persian Gulf. Naval Environmental Prediction Research Facility, Monterey, California. Report: TR 79-06. <https://apps.dtic.mil/dtic/tr/fulltext/u2/a077727.pdf>
- Rajeevan, M., Unnikrishnan, C. K., Bhate, J., Niranjana Kumar, K., & Sreekala, P. P. (2012). Northeast monsoon over India: variability and prediction. *Meteorological Applications*, 19(2), 226-236. <https://doi.org/10.1002/met.1322>
- Remya, P.G., Vishnu, S., Praveen Kumar, B., Balakrishnan Nair, T.M., Rohith, B. (2016). Teleconnection between the North Indian Ocean high swell events and meteorological conditions over the Southern Indian Ocean. *Journal of Geophysical Research (Oceans)*, 121(10), 7476-7494.
- Saha, S., Moorthi, S., Wu, X., Wang, J., Nadiga, S., Tripp, P., ... Ek, M. (2014). The NCEP climate forecast system version 2. *Journal of Climate*, 27(6), 2185-2208. <https://doi.org/10.1175/JCLI-D-12-00823.1>
- Samiksha, S. V., Vethamony, P., Aboobacker, V. M., & Rashmi, R. (2012). Propagation of Atlantic Ocean swells in the north Indian Ocean: a case study. *Natural Hazards and Earth Systems Sciences*. 12, 3605-3615. doi:10.5194/nhess-12-3605-2012
- Samiksha, S. V., Vinod Kumar, K., Vethamony, P. (2014). Impact of shamal winds and swells on the coastal currents along the west coast of India. *Indian Journal of Marine Sciences*, 43(07), 1236-1240.
- Sharp, E., Dodds, P., Barrett, M., & Spataru, C. (2015). Evaluating the accuracy of CFSR reanalysis hourly wind speed forecasts for the UK, using in situ measurements and geographical information. *Renewable Energy*, 77, 527-538. <https://doi.org/10.1016/j.renene.2014.12.025>

- Tolman, H. L. the WAVEWATCH III® Development Group (2014), User Manual and System Documentation of WAVEWATCH III® version 4.18. Technical Note 316, NOAA/NWS/NCEP/MMAB.
<http://polar.ncep.noaa.gov/waves/wavewatch/manual.v4.18.pdf>
- Tucker, M.J. (1989). Interpreting directional data from large pitch-roll-heave buoys. *Ocean Engineering*, 16(2), 173-192. [https://doi.org/10.1016/0029-8018\(89\)90004-8](https://doi.org/10.1016/0029-8018(89)90004-8)
- Vethamony, P., Aboobacker, V. M., Menon, H. B., Kumar, K. A., & Cavaleri, L. (2011). Superimposition of wind seas on pre-existing swells off Goa coast. *Journal of Marine Systems*, 87(1), 47-54. <http://dx.doi.org/10.1016/j.jmarsys.2011.02.024>
- Vinodkumar, K., Seemanth, M., Vethamony, P., Aboobacker, V.M. (2014). On the spatial structure and time evolution of shamal winds over the Arabian Sea – a case study through numerical modelling. *International Journal of Climatology*, 34, 2122-2128. <https://doi.org/10.1002/joc.3819>
- Yu, Y., Notaro, M., Kalashnikova, O.G., Garay, M.J. (2016). Climatology of summer shamal winds in the Middle East. *Journal of Geophysical Research-Atmosphere*, 121: 289-305. <https://doi.org/10.1002/2015JD024063>

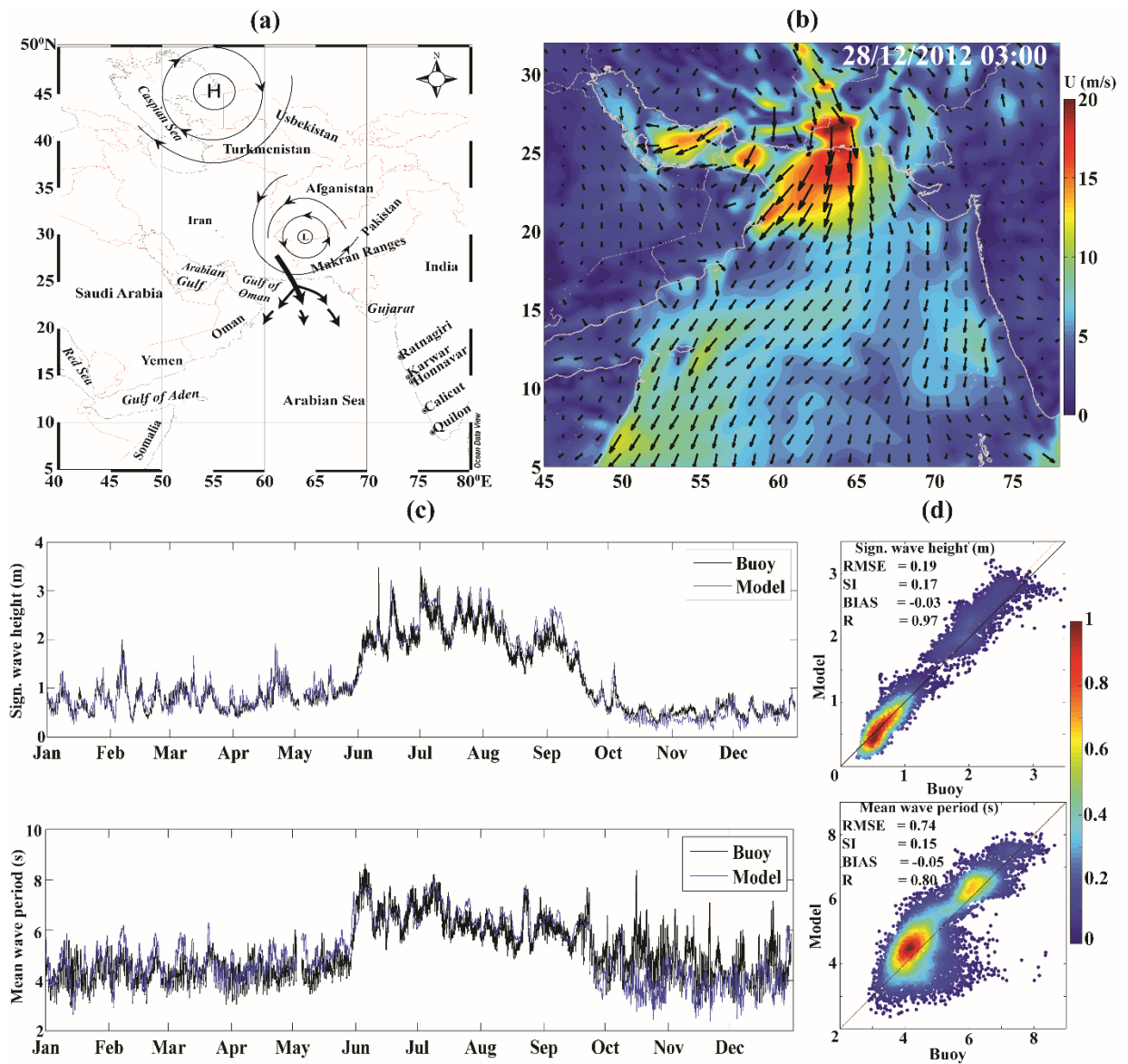


Figure 1. (a) A representative image on the development of the northerly LLJ and its transformation as makran winds (b) Snapshot of makran winds in the Arabian Sea and (c) – (d) Comparison between measured and modelled significant wave height and mean wave period.

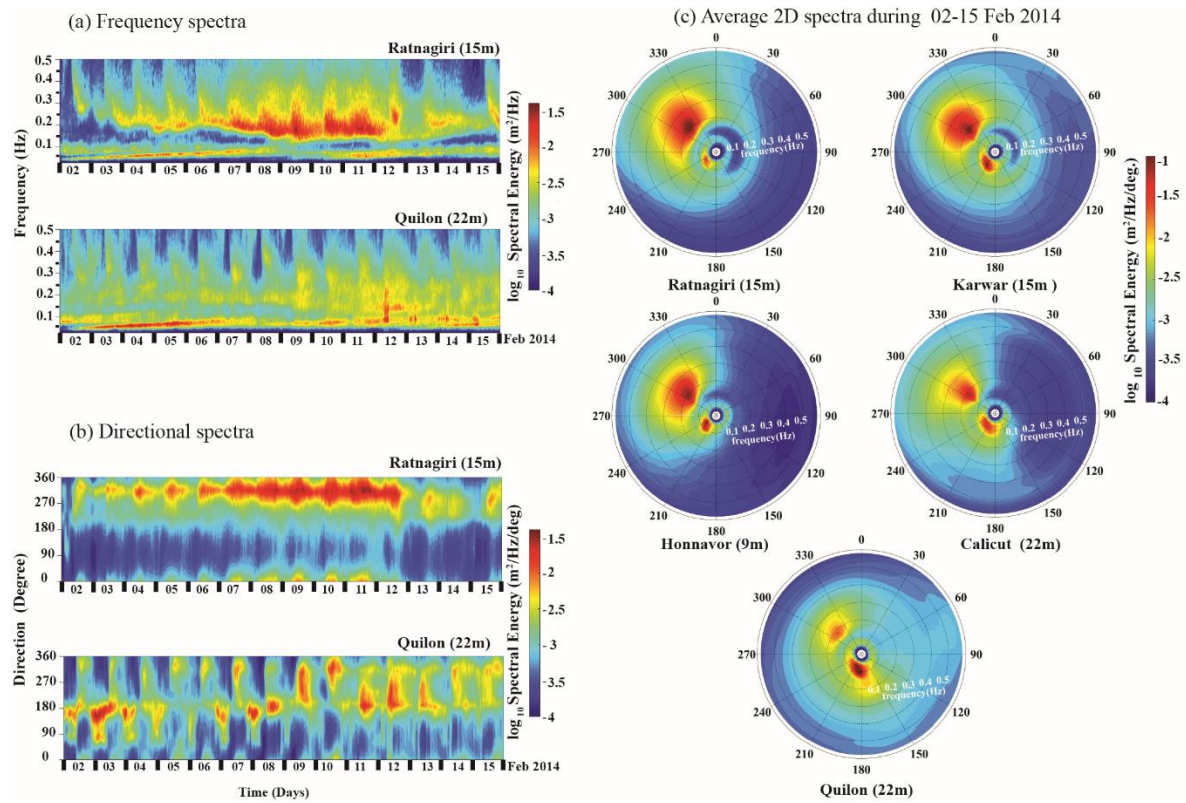


Figure 2. (a) Time series normalized frequency spectra, (b) time series normalized directional spectra and (c) average 2D spectra along the west coast of India during 02 – 15 Feb 2014.

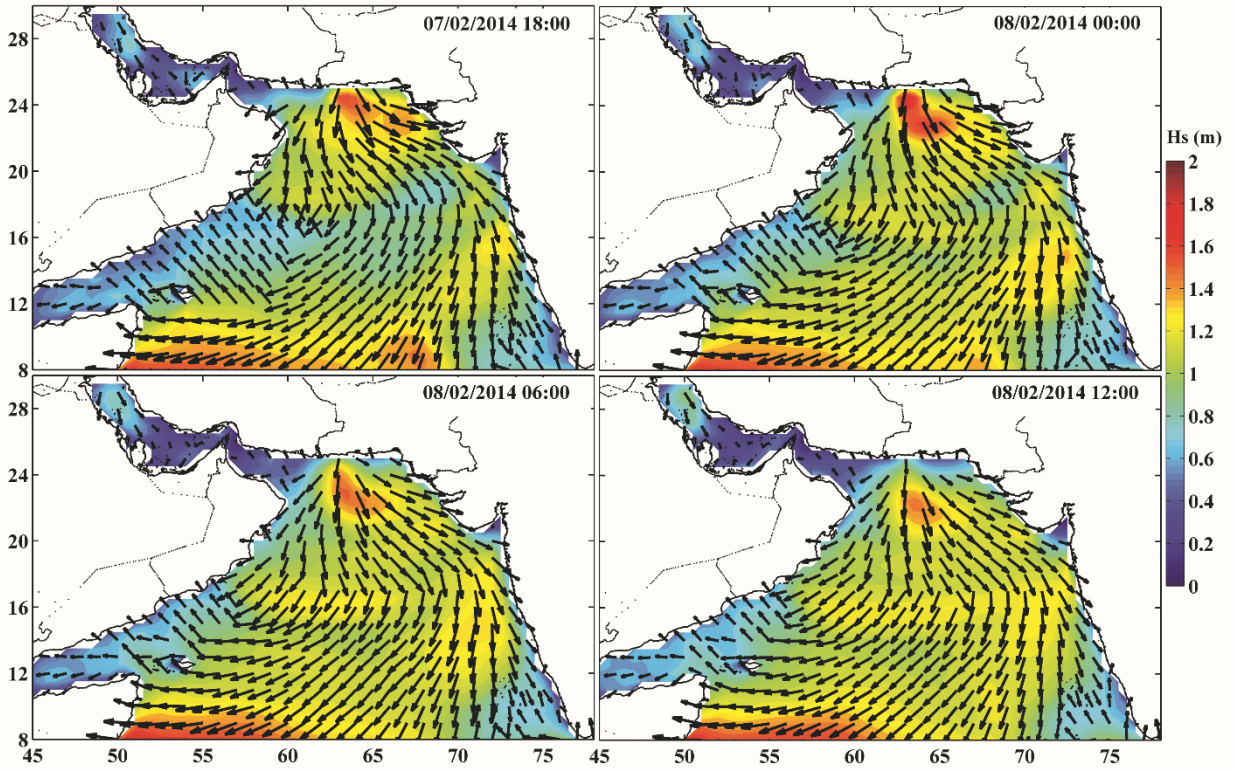


Figure 3 Snapshots of makran significant wave heights (colour shades) and dominant wave directions (black vectors) in the Arabian Sea during 07-08 Feb 2014.

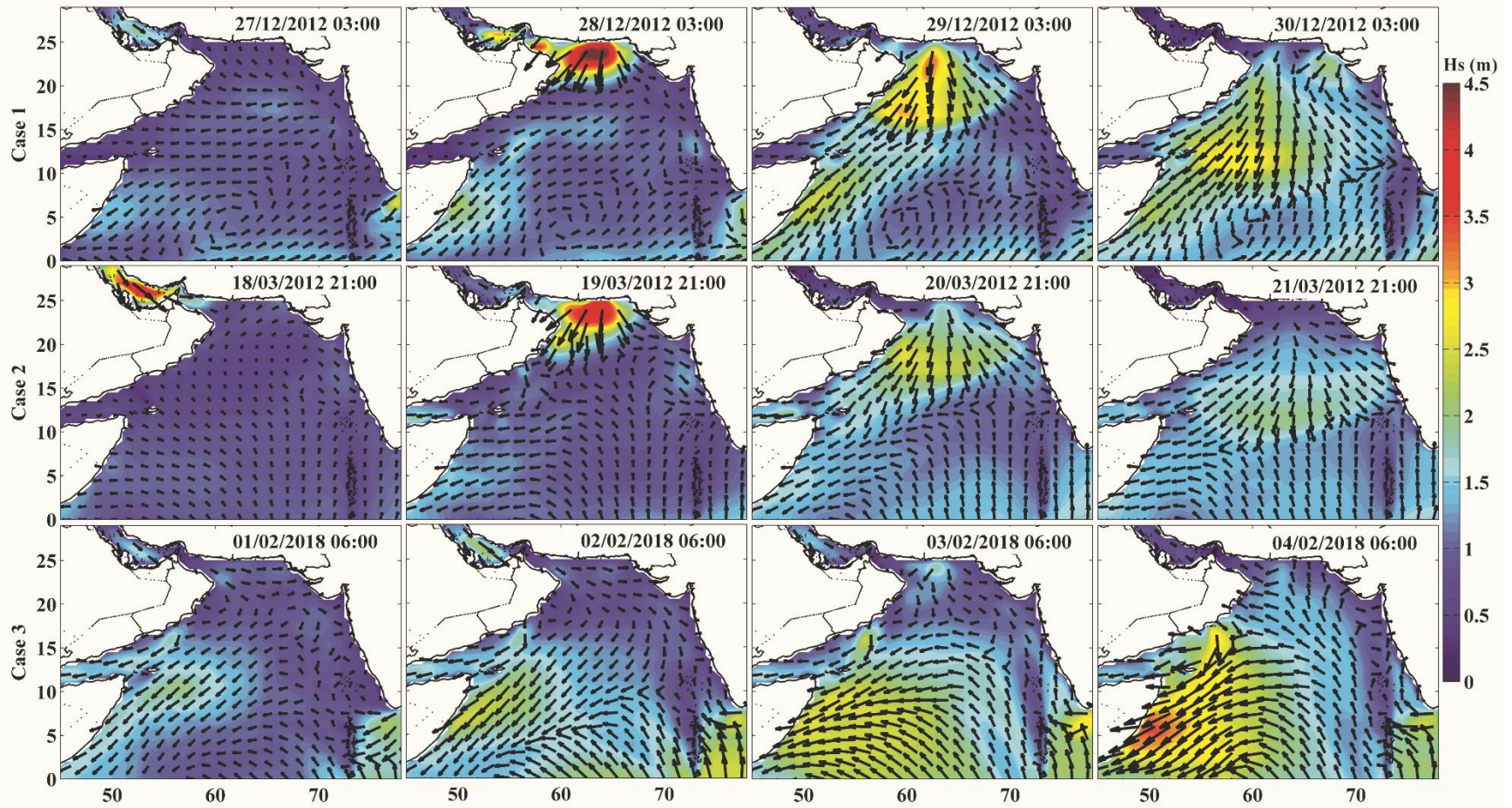


Figure 4 Snapshots of makran swells corresponds to three typical cases: (a) Case1: Independent makran swells, (b) Case2: Dominance of makran swells over shamal swells and (c) Case3: Co-existence of makran and shamal swells.